Int. J. Nano Dimens., 12 (4): 335-342, Autumn 2021

ORIGINAL ARTICLE

Polarizability and second hyperpolarizability of $M@B_{24}N_{24}$ cages (M=Li, Na and K)

Mojtaba Yaghobi*, Misagheh Ahmadi

Departments of Physics, Ayatollah Amoli Branch, Islamic Azad University, Amol, Iran

Received 12 March 20; revised 21 April 2021; accepted 01 May 2021; available online 09 May 2021

Abstract

By applying B3LYP/6-31G* time dependent density functional level of theory and sum-over-state (SOS) approach, the static and frequency dependent polarizability and second hyperpolarizability properties of the $B_{24}N_{24}$, $Li@B_{24}N_{24}$, $Na@B_{24}N_{24}$ and $K@B_{24}N_{24}$ cages have been studied. The polarizability and second hyperpolarizability properties of $B_{24}N_{24}$ cage have been studied by considering effects of *Li, Na* and *K* atoms encapsulation in the $B_{24}N_{24}$ cage. The type and encapsulation of *M* atom can greatly impress on polarizabilities and second hyperpolarizabilities values of $B_{24}N_{24}$ cage. As, highest peak value of second hyperpolarizabilities for $K@B_{24}N_{24}$ is about 23 times larger than that of the $B_{24}N_{24}$, $Li@B_{24}N_{24}$ and $Na@B_{24}N_{24}$ cages. It seems that $M@B_{24}N_{24}$ cages can be used to produce the semiconductors with various band gaps.

Keywords: *ab initio; B-N Material; Cage; Density Functional; Endoedral; Sum-over-state.*

How to cite this article

M. Yaghobi, M. Ahmadi Polarizability and second hyperpolarizability of $M@B_{24}N_{24}$ cages (M=Li, Na and K). Int. J. Nano Dimens., 2021; 12(4): 335-342.

INTRODUCTION

In recent years, Nano- boron- nitride materials such as graphene, BN fullerene-like and nanotubes have been attracting much attention due to their excellent and unique electrical and optical properties in the fields of material science and engineering. Many photon effects are energy dependent and find numerous applications in technology, telecommunication, medicine, etc [1-8]. Mass spectrum for BN clusters in pyridine solution demonstrated the existence of *(BN)n* (n=12-80) clusters [5]. These materials are better than nanotubes carbons in some cases [9, 10]. The possible candidate structures for the *BN* cages reported theoretically or synthesized in experiments [1, 10–20]. The results showed that the most stable isomer of $B_{24}N_{24}$ is the structure with 2 octagons, 16 hexagons and 8 squares in S8 symmetry [21].

The endohedral metallofullerenes, fullerenes with encapsulated metal atoms were discovered after the discovery of fullerenes [22–24]. A metafullerene is an endohedral fullerene that a metal atom is placed into the fullerenes. The hollow structure of this material can entangle small materials such as Helium, while there is no reaction with fullerenes molecule. In fact, the inside of fullerenes majority are very big and they can entangle all the elements in periodic table. Through fullerenes doping, they can be electrically conductive, semi-conductive or superconductive. Endohedral *BN* clusters [Yx@(BN)n] with yttrium atoms encapsulated inside the BN clusters were detected [5].

Density-functional theory (DFT) as a computational quantum mechanical modelling method is used in physics, chemistry and materials science. This theory studies the electronic structure of many-body systems in particular atoms, molecules and the condensed phases. Using functionals, i.e. functions of another function in this theory, the properties of a many-electron system can be calculated. In the case of DFT, these

* Corresponding Author Email: *m.yaghoubi@iauamol.ac.ir*

are functionals of the spatially dependent electron density. In this work, the most stable $B_{24}N_{24}$ cage is considered to investigate polarizability and second hyperpolarizability properties of $M@B_{24}N_{24}$ cages using B3LYP/6-31G* time dependent density functional level of theory. $M@B_{24}N_{24}$ cages are not organic molecule therefore B3LYP/6-31G** method is not used in calculation of this work.

Computational details

In this work, the results were obtained by using the B3LYP/6-31G* level of time dependent density functional theory (TDDFT) with the Gaussian 98 quantum chemistry software package [21]. The pervious works indicated B3LYP/6-31G method is quite adequate for the different nanostructures [16-20, 22-23]. Minimum of total potential energy of endohedral complexes of the $B_{24}N_{24}$, $Li@B_{24}N_{24}$, $Na@B_{24}N_{24}$ and $K@B_{24}N_{24}$ cages study by full geometry optimization with B3LYP/6-31G* method.

The polarizabilities and hyperpolarizabilities additively from the contributions of different electronic excited states in a given molecule can be calculated using the sum-over-states (SOS) method. Subsequent analysis of the main excited configurations contributing to the relevant excited states allows characterizing the orbitals involved in the linear and nonlinear optical response.

Polarizability (α) and second hyperpolarizability (γ) can calculate as [24, 25]:

$$\alpha_{i,j}(-\omega;\omega) = P(-\omega_P;\omega_1)\sum_{\boldsymbol{b}}\frac{\langle a|r_i|b\rangle\langle b|r_j|a\rangle}{(\varepsilon_b-\varepsilon_a-\omega_1-i\eta)} \quad (1)$$

And

$$\gamma_{ijkl}(-\omega_P;\omega_1,\omega_2,\omega_3) = P(-\omega_P;\omega_1,\omega_2,\omega_3)$$
$$\times\left\{\sum_{arst}\frac{\langle a|\mu_i|r\rangle\langle r|\mu_l|s\rangle\langle s|\mu_k|t\rangle\langle t|\mu_j|a\rangle}{(\varepsilon_r-\varepsilon_a-\omega_p-i\eta)(\varepsilon_s-\varepsilon_a-\omega_1-\omega_2-i\eta)(\varepsilon_t-\varepsilon_a-\omega_1-i\eta)}\right.$$
$$+\sum_{abcr}\frac{\langle a|\mu_i|r\rangle\langle b|\mu_j|a\rangle\langle c|\mu_k|b\rangle\langle r|\mu_l|c\rangle}{(\varepsilon_r-\varepsilon_a-\omega_p-i\eta)(\varepsilon_r-\varepsilon_b-\omega_1-\omega_2-i\eta)(\varepsilon_r-\varepsilon_c-\omega_1-i\eta)}$$
$$-\sum_{abrs}\frac{\langle a|\mu_i|r\rangle\langle b|\mu_l|a\rangle\langle c|\mu_j|b\rangle\langle r|\mu_k|c\rangle}{(\varepsilon_r-\varepsilon_a-\omega_p-i\eta)(\varepsilon_s-\varepsilon_a-\omega_1-\omega_2-i\eta)(\varepsilon_s-\varepsilon_b-\omega_1-i\eta)}$$
$$-\sum_{abrs}\frac{\langle a|\mu_i|r\rangle\langle b|\mu_k|a\rangle\langle c|\mu_j|b\rangle\langle r|\mu_l|c\rangle}{(\varepsilon_r-\varepsilon_a-\omega_p-i\eta)(\varepsilon_r-\varepsilon_b-\omega_1-\omega_2-i\eta)(\varepsilon_s-\varepsilon_b-\omega_1-i\eta)}$$
$$\left.-\sum_{abrs}\frac{\langle a|\mu_i|r\rangle\langle b|\mu_k|a\rangle\langle c|\mu_l|b\rangle\langle r|\mu_j|c\rangle}{(\varepsilon_r-\varepsilon_a-\omega_p-i\eta)(\varepsilon_r-\varepsilon_b-\omega_2-i\eta)(\varepsilon_s-\varepsilon_a-\omega_1-i\eta)}\right\}$$

where *a, b* and c (*r, s* and *t*) indicate the occupied (virtual) molecular orbitals and μ_i is electric dipole transition moments. The lifetime broadening factors is selected 0.0168 and 0.01eV for the polarizability (α) and second (γ) hyperpolarizability, respectively. $\langle\alpha\rangle$ is exciton energy.

Molecular orbitals and molecular orbital energies can study by follow eigenvalue problem [26]:

$$H_{(n_1,n_2),(n_3,n_4)} = (\varepsilon_{n_2}-\varepsilon_{n_1})\delta_{n_1,n_3}\delta_{n_2,n_4} + H'_{(n_1,n_2),(n_3,n_4)} \quad (3)$$

In calculations, we set H'=0. In above equation $(\varepsilon_{n_2}-\varepsilon_{n_1})$ is the transition energy and ε_{n_i} is eigenvalues (ε_{n_i}) of TDDFT.

The average polarizability and second hyperpolarizability can calculate as:

$$\alpha = \frac{1}{3}\sum_i \alpha_{ii}(-\omega,\omega) \quad (4)$$

$$\gamma = \frac{1}{15}\sum_i\sum_j(2\gamma_{iijj}(-3\omega;\omega,\omega,\omega)+\gamma_{ijji}(-3\omega;\omega,\omega,\omega)) \quad (5)$$

where *i* and *j* represent either *x, y* and *z* in Cartesian coordinates. A more direct comparison with experiment is possible through $\langle\gamma\rangle$ which reads:

$$\langle\alpha\rangle = \sqrt{\alpha_R^2+\alpha_I^2} \quad (6)$$

$$\langle\gamma\rangle = \sqrt{\gamma_R^2+\gamma_I^2} \quad (7)$$

Here *R* and *I* indexes indicate real and imaginary components [24, 25].

RESULTS AND DISCUSSION

In this study, polarizability and second hyperpolarizability properties of the $B_{24}N_{24}$, $Li@B_{24}N_{24}$, $Na@B_{24}N_{24}$ and $K@B_{24}N_{24}$ cages have been investigated for the case of the M atoms at center of $B_{24}N_{24}$ cage by the TDDFT-B3LYP/6-31G* level of theory. Figs. 1(a-d) show optimized structures of the $B_{24}N_{24}$, $Li@B_{24}N_{24}$, $Na@B_{24}N_{24}$ and $K@B_{24}N_{24}$ cages, respectively. Corresponding with Figs. 1, the studied structures of $M@B_{24}N_{24}$ cages are created by the encapsulation doping on $B_{24}N_{24}$ cage. The $B_{24}N_{24}$ fullerene consists of with 2 octagons (Fig. 2(a), 16 hexagons (Fig. 2 (b)) and 8 squares (Fig. 2(c)) in S8 symmetry.

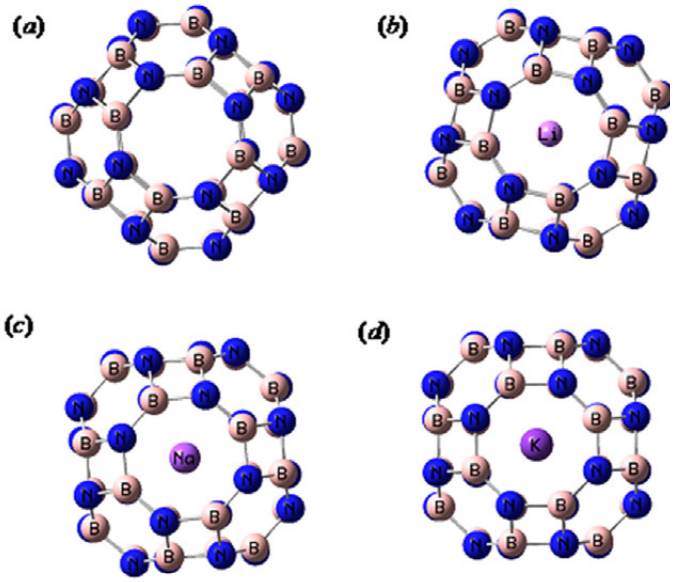

Fig.1. Optimized structural of (a) $B_{24}N_{24}$, (b) $Li@B_{24}N_{24}$, (c) $Na@B_{24}N_{24}$ and (d) $K@B_{24}N_{24}$ cages.

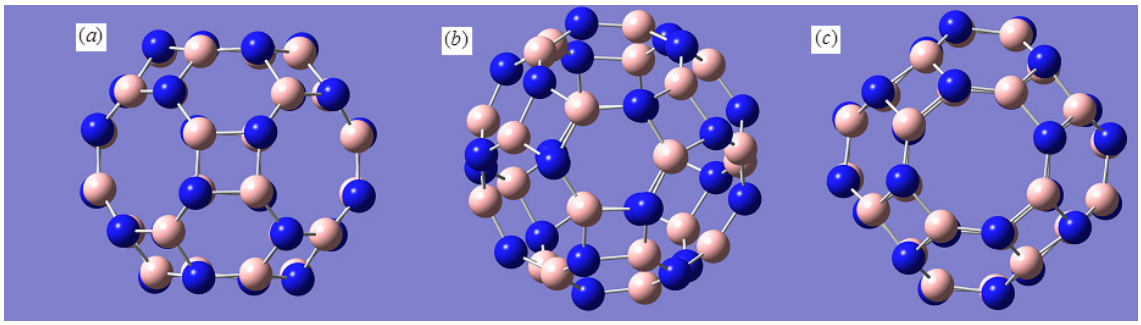

Fig.2. The structure of (a) octagons, (b) hexagons and (c) squares in $B_{24}N_{24}$ cage.

Mean static polarizabilities ($\langle\alpha\rangle$), band gaps between HOMO and LUMO and the position of the first peak (ω_1) against energy of $M@B_{24}N_{24}$ cages have been indicated in Table 1. Table 1 show $B_{24}N_{24}$ cage is an insulator and its wide energy gap (ΔE) is 5.9 *eV*. For the $M@B_{24}N_{24}$ cages, the energy gaps varies between 2.25 eV, 1.87 and 0.99 eV for $Li@B_{24}N_{24}$, $Na@B_{24}N_{24}$ and $K@B_{24}N_{24}$, respectively. Therefore, the reactivity of $Li@B_{24}N_{24}$, $Na@B_{24}N_{24}$ and $K@B_{24}N_{24}$ cages is more than $B_{24}N_{24}$ cage due to encapsulation *of M* atom. When *M* atom locates into $B_{24}N_{24}$ cage, the change of energy gap of $B_{24}N_{24}$ cage is corresponding with the increasing ionic radius of *M* atom. Also, values of the excitation energies of $M@B_{24}N_{24}$ are smaller than that for $B_{24}N_{24}$ cage. The optical properties of $M@B_{24}N_{24}$ is corresponding to its energy gap. Thus, it seems that $M@B_{24}N_{24}$ cages can be used to produce the semiconductors with various band gaps. The mentioned results are in accordance to similar systems [12-17].

From Table 1 is seen that the $\langle\alpha\rangle$ of $M@B_{24}N_{24}$ cages are the bigger than that of $B_{24}N_{24}$. The $\langle\alpha\rangle$ of $K@B_{24}N_{24}$ is bigger than that for $Li@B_{24}N_{24}$ and $Na@B_{24}N_{24}$ cages. This is due to that excitation energies are in the denominator of the expression for the polarizability and smaller excitation energies result in larger values for the polarizability [12-15]. The pervious results for substituted doped fullerenes are in accordance to these results [12-17].

From mean static second polarizabilities ($\langle\gamma\rangle$) in Tables 1, it is seen that second polarizability

value of $K@B_{24}N_{24}$ cage is about 23 times larger than that of $B_{24}N_{24}$ cage. Therefore, encapsulation of *M* atom increases second polarizability value which is similar to the theoretical prediction for doped fullerenes [12-17].

Figs. 3(a), (b), (c) and 3 (d) show the polarizability dispersions of $B_{24}N_{24}$, $Li@B_{24}N_{24}$, $Na@B_{24}N_{24}$ and $K@B_{24}N_{24}$ cages against energy, respectively. Results indicate that major peaks values of polarizabilities of $B_{24}N_{24}$ cage reduce respect to that of the $M@B_{24}N_{24}$ cages. The first peak position of polarizability of $M@C_{59}X$ cages locates in lower frequencies relative to that for $B_{24}N_{24}$ cage. The results present that the polarizability dispersion depends on the *M* atom type and can been controllable by selection of the endohedral elements.

Second hyperpolarizabilities ($\langle\gamma\rangle$) spectra of $B_{24}N_{24}$ and $M@B_{24}N_{24}$ cages are shown in Figs. 4 (a)-(d) against energy. The second polarizability spectra of $B_{24}N_{24}$ in comparison with that of $M@B_{24}N_{24}$ cage show the big peaks with very much smaller. Similar with the polarizability dispersion, the first peak position of second hyperpolarizabilities of $M@C_{59}X$ cages locates in lower frequencies relative to that for $B_{24}N_{24}$ cage. The $K@B_{24}N_{24}$ cage has the highest peak of second hyperpolarizabilities with respect to

Table 1. Static different components of polarizability (in esu), the first peak position (ω_1, in eV) and the band gap (E_g, in eV) with respect to energy and Static different components of second hyperpolarizability (in 10^{-34} esu) for $B_{24}N_{24}$, $Li@B_{24}N_{24}$, $Na@B_{24}N_{24}$ and $K@B_{24}N_{24}$.

	$B_{24}N_{24}$	$Li@B_{24}N_{24}$	$Na@B_{24}N_{24}$	$K@B_{24}N_{24}$
E_g	5.9	2.25	1.87	.099
$\langle\alpha\rangle$	919	2045	2063	2174
ω_1	6.2	2.82	2.60	1
$\langle\gamma\rangle$	2.45	4.56	4.8	56.71

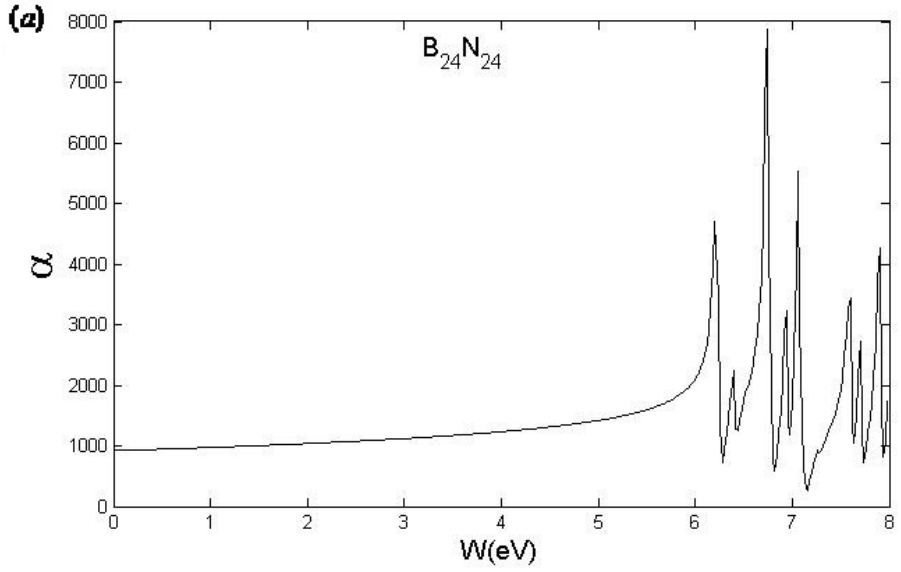

Fig. 3. Mean polarizability against energy (*eV*) (in 10^3 esu) for cages (a) $B_{24}N_{24}$, (b) $Li@B_{24}N_{24}$, (c) $Na@B_{24}N_{24}$ and (d) $K@B_{24}N_{24}$.

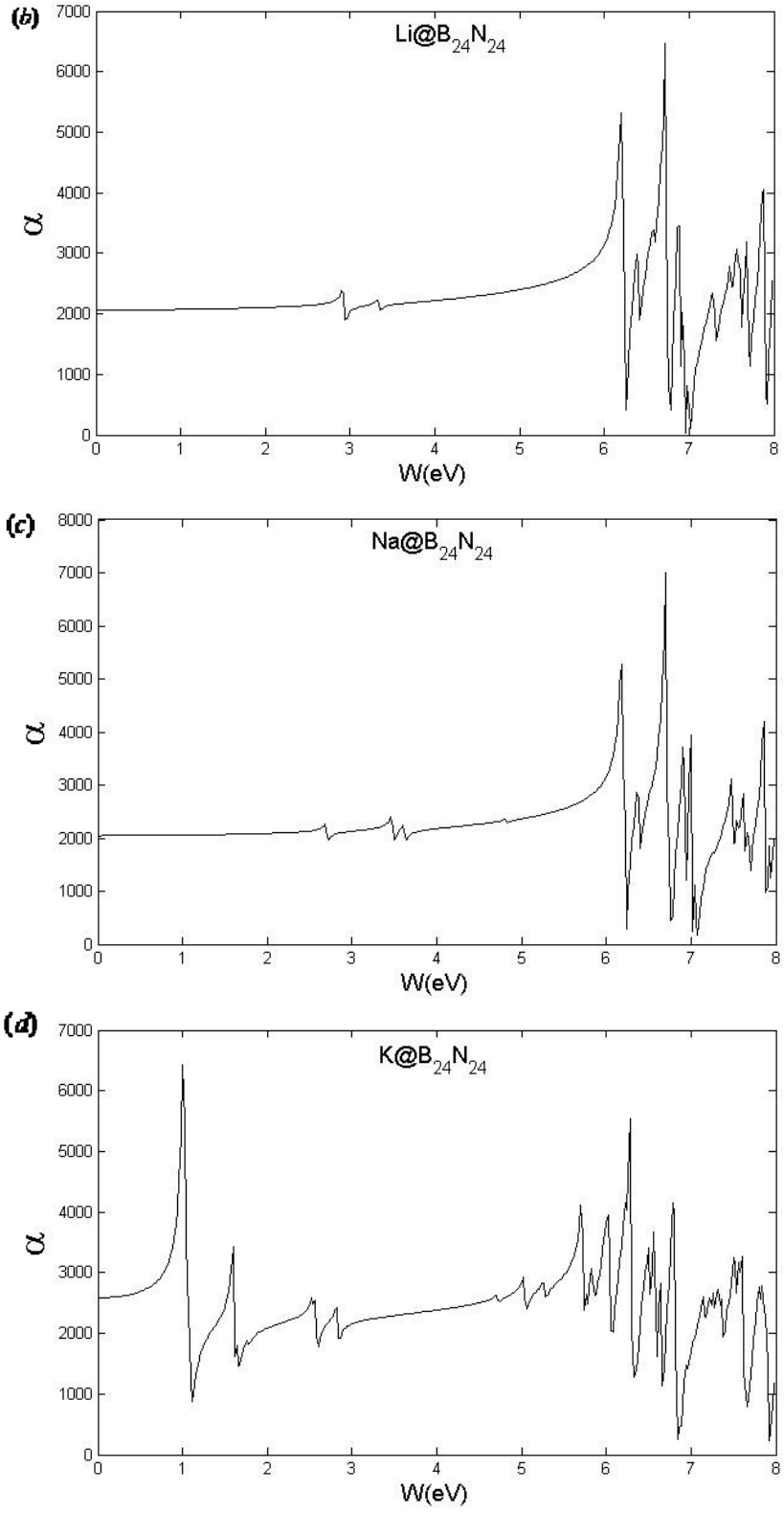

Continued Fig. 3. Mean polarizability against energy (*eV*) (in 10^3 esu) for cages (a) $B_{24}N_{24}$, (b) $Li@B_{24}N_{24}$, (c) $Na@B_{24}N_{24}$ and (d) $K@B_{24}N_{24}$.

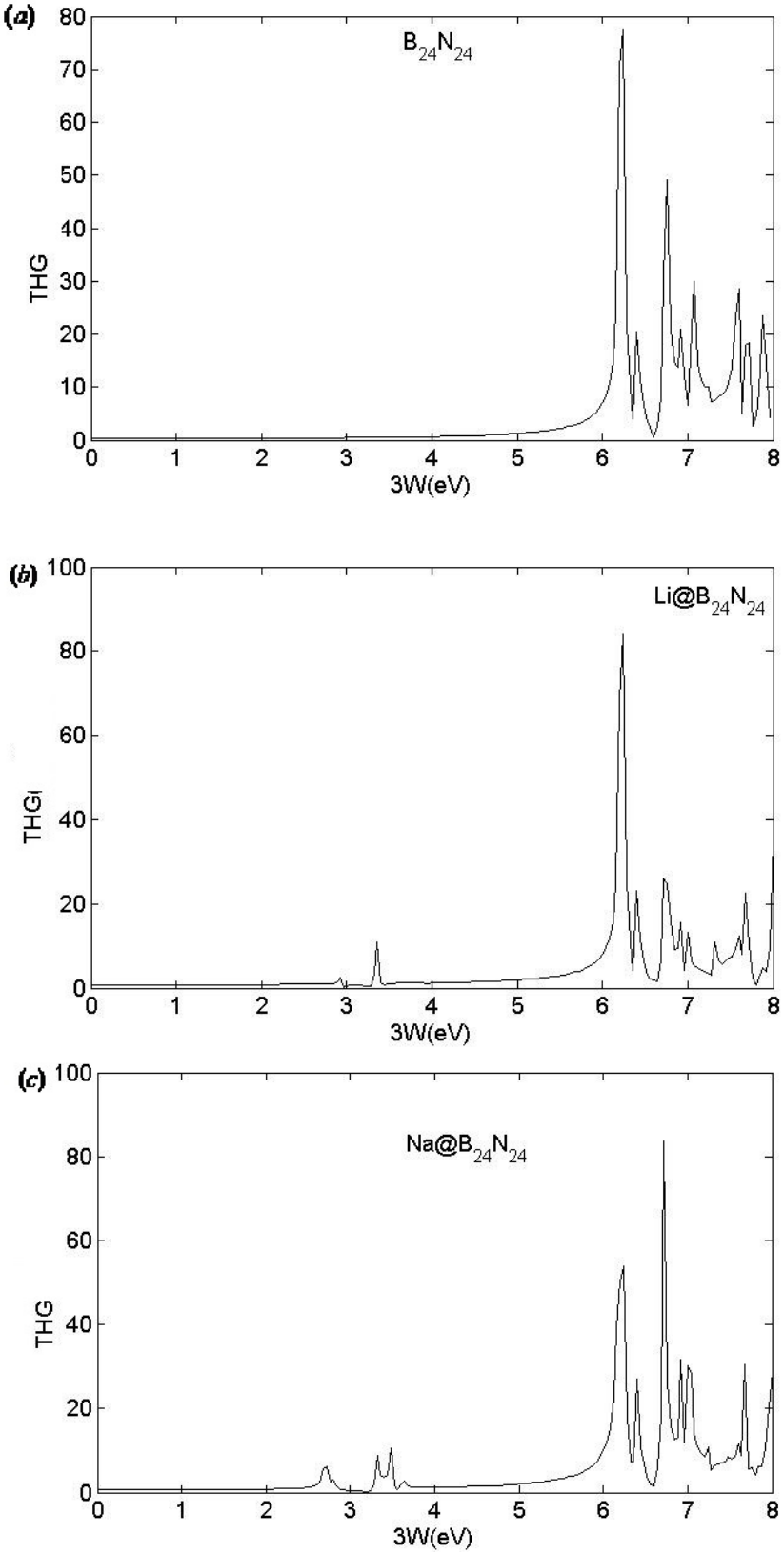

Fig. 4. Mean second polarizability against energy (*eV*) (in 10^{-34} esu) for cages (a) $B_{24}N_{24}$, (b) $Li@B_{24}N_{24}$, (c) $Na@B_{24}N_{24}$ and (d) $K@B_{24}N_{24}$.

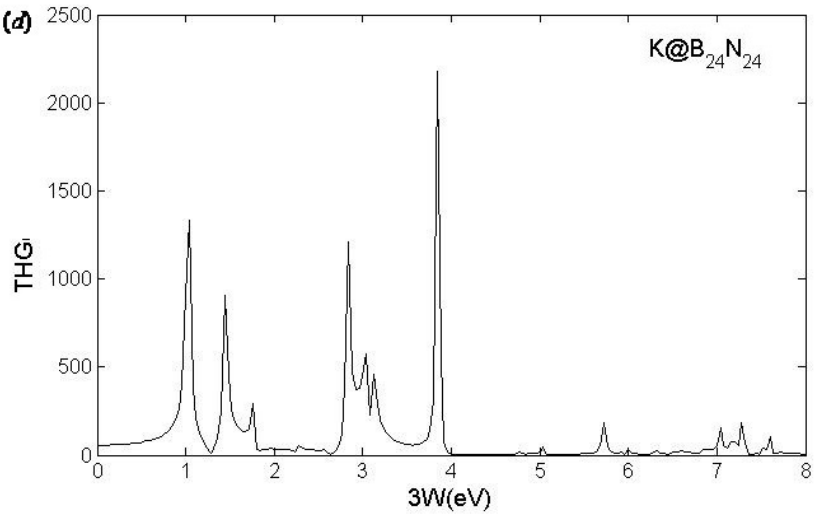

Continued Fig. 4. Mean second polarizability against energy (*eV*) (in 10^{-34} esu) for cages (a) $B_{24}N_{24}$, (b) $Li@B_{24}N_{24}$, (c) $Na@B_{24}N_{24}$ and (d) $K@B_{24}N_{24}$.

$B_{24}N_{24}$, $Li@B_{24}N_{24}$ and $Na@B_{24}N_{24}$ cages. The highest peak value of $K@B_{24}N_{24}$, $Na@B_{24}N_{24}$ and $Li@C_{59}X$ molecules are about 30, 1.2 and 1.1 times larger than that of $B_{24}N_{24}$ molecule, respectively. For energies in range 0.0 to 8.0 eV, comparison of Fig. 3(a) with Fig. 4(a) indicates there are not the two and three-photon peaks for $B_{24}N_{24}$ molecules. These results are in accordance with others work [27-31]. Also, comparisons of Fig. 3(b) with Fig. 4 (b) and Fig. 3(c) with Fig. 4(c) indicate there are not three-photon peaks for $Li@B_{24}N_{24}$ and $Na@B_{24}N_{24}$ cages for energies in range 0.0 to 8.0 eV. The two-photon peaks are observed in 3ω=6 and 6.8 *eV* for $Li@B_{24}N_{24}$ and 3ω= 7 and 7.2 *eV* for $Na@B_{24}N_{24}$ cage. The comparison of Fig. 2(d) with Fig. 3(d) indicates there are three-photon and two-photon peaks for $K@B_{24}N_{24}$ cage for energies in range 0.0 to 8.0 eV. The two-photon intensities of $K@B_{24}N_{24}$ are seen at 3ω=3.00, 3.2, 3.8, 5and 6 eV. Also, the tree-photon intensities of $K@B_{24}N_{24}$ are seen at 3ω=4.80, 5, 7.5and 7.7 eV.

The highest peaks of $K@B_{24}N_{24}$ respect to $B_{24}N_{24}$, $K@B_{24}N_{24}$ and $Na@B_{24}N_{24}$ cages can be explained by the following two effects. One is the large single photon intensities in same energies as shown in Fig. 2 for $K@B_{24}N_{24}$, and the other is double resonance enhancement occurring .These results are similar to other doped systems results [10, 27-31]. For example, the Eleanor et. al. calculations indicated that $Li@C_{60}$ has the second hyperpolarizability 3-5 times larger than that of pure C_{60} [28].

We propose following explanation for mentioned behaviors. The transition energy and transition matrix element between one-electron states are factors that can impress on polarizabilities and second hyperpolarizabilities spectra. Overall, polarizabilities and second hyperpolarizabilities depend on the degeneracy of energy levels, band gap and symmetry properties of cage. The structure, bond lengths and gap energy of cage change when *M* atom locates into the $B_{24}N_{24}$ cage. It indicates that *M* atom type effects on cage structure and symmetric properties. Thereby, *M* atom type and encapsulation change the cage symmetry and therewith changes electronic structures and polarizabilities and second hyperpolarizabilities spectra of $B_{24}N_{24}$ cages.

CONCLUSIONS

Effects of encapsulation and type of *M* atom on the polarizability and second hyperpolarizability of $B_{24}N_{24}$ cage studied using the TDDFT-B3LYP/6-31G* level. Furthermore, the SoS approximation is applied for study of the polarizability and hyperpolarizability of the $B_{24}N_{24}$, $Li@B_{24}N_{24}$, $Na@B_{24}N_{24}$ and $K@B_{24}N_{24}$ cages. The structural, symmetric properties, the polarizability and hyperpolarizability spectra of the $B_{24}N_{24}$ cage change by *M* atom encapsulation. Also, the static polarizability and hyperpolarizability of the $M@B_{24}N_{24}$ molecules is bigger than that of

the $B_{24}N_{24}$ cage. Our calculations conclude that $M@B_{24}N_{24}$ cages are interesting candidates for application in optoelectronics.

CONFLICT OF INTERESTS

There is no conflict of interest.

REFERENCES

[1] Munn R. W., Ironside C. N., (1993), *Principles and Applications of Nonlinear Optical Materials,* London: Chapman and Hall.

[2] Han L. A., Chen C. L., (2012), Transport properties and laser irradiation effect in $Ca_{0.8}Ce_{0.2}MnO_3$ film. *Indian J. Phys.* 86: 877-880.

[3] Gogoi A., Ahmed G. A., Choudhury A., (2009), Nanoparticle size characterization by laser light scattering. *Indian J. Phys.* 83: 473-477.

[4] Ahmadi R., Pirahan Foroush M., (2014), Fullerene effect on chemical properties of antihypertensive clonidine in water phase. *Annals of Military Health Sci. Res.*12: 39-43.

[5] Blackmore K. J., Lal N., Ziller J. W., Heyduk A. F., (2008), Catalytic reactivity of a zirconium(IV) redox-active ligand complex with 1, 2-diphenylhydrazine. *J. Am. Chem. Soc.* 130: 2728–2729.

[6] Yaghobi M., (2014), Effect of carbon doping on polarizability and second hyperpolarizability of $B_{12}N_{12}$ cage, *Indian J. Phys.* 88: 237-242.

[7] Marder S. R., Torruellas W. E., Blanchard-Desce M., Ricci V., Stegeman G. I., Gilmour S., Bredas J. –L., Li J., Bublitz G. U., Boxe S. G., (1997), Large molecular third-order optical nonlinearities in polarized carotenoids. *Science.* 276: 1233-1236.

[8] Dresselhaus M. S., (1996), *Science of Fullerenes and Carbon Nanotubes: Their Properties and Applications,* New York: Academic Press.

[9] Heath J. R., Brien S. C. O., Zhang Q., Liu Y., Curl R. F., Tittel F. K., Smalley R. E., (1985), Lanthanum complexes of spheroidal carbon shells. *J. Am. Chem. Soc.* 107: 7779-7780.

[10] Chai Y., Guo T., Jin C., Haufler R. E., Chibante L. P. F., Fure J., Wang L., Alford J. M., Smalley R. E., (1991), Fullerenes with metals inside. *J. Phys. Chem.* 95: 7564–7568.

[11] Johnson R. D., de Vries M. S., Salem J. R., Bethunde D. S., Yannoni C. S., (1992), Electron paramagnetic resonance studies of lanthanum-containing C82. *Nature*. 355: 239-244.

[12] Andreoni W., Gygi F., Parrinello M., (1992), Impurity states in doped fullerenes: $C_{59}B$ and $C_{59}N$. *Chem. Phys. Lett.* 190: 159-162.

[13] Hummelen J. C., Bellavia-Lund C., Wudl F., (1999), *Fullerenes and related structures* (eds) A Hirsch , Berlin, Heidelberg: Springer.

[14] Hummelen J. C., Knight B., Pavlovich J., Gonzalez R., Wudl F., (1995), Isolation of the heterofullerene C59N as Its dimer $(C59N)_2$. *Science* 269: 1554-1558.

[15] Forrol L., Mihaly L., (2001), Electronic properties of doped fullerenes. *Rep. Prog. Phys.* 64: 649-708.

[16] Hou J. Q., Kang H. S., (2007), DFT study on the stabilities of the heterofullerenes $Sc_3N@C_{67}B$, $Sc_3N@C_{67}N$, and $Sc_3N@C_{66}BN$. *J. Phys. Chem. A*. 111: 1111-1116.

[17] Stevenson S., Rice G., Glass T., Harich K., Cromer F., Jordan M. R., Craft J., Hadju E., Bible R., Olmstead M. M., Maitra K., Fisher A. J., Balch A. L., Dorn H. C., (1999), Small-bandgap endohedral metallofullerenes in high yield and purity. *Nature*. 401: 55-57.

[18] Yaghobi M., Adabinezhad A. R., (2016), Structural and optical properties of the $M@C_{59}X$ cages (X=N, B and M=Li, Na). *Pramana J. Phys*. 86: 109–116.

[19] Juárez R., Salazar Villanueva M., Cortés-Arriagada D., Chigo Anota E., (2019), Fullerene-like boron nitride cages BxNy (x+y=28): Stabilities and electronic properties from density functional theory computation. *J. Mol. Model*. 25: 21-27.

[20] Fu W., Zhang J., Fuhrer T., Champion H., Furukawa K., Kato T., Mahaney J. E., Burke B. G., Williams K. A., Walker K., Dixon C., Ge J., Shu C., Harich K., Dorn H. C., (2011), Gd2@C79N: Isolation, characterization, and mono adduct formation of a very stable hetero fullerene with a magnetic spin state of S = 15/2. *Am. Chem. Soc*. 133: 9741-9750.

[21] Frisch M. J., Trucks G. W., Schlegel H. B., Scuseria G. E., Robb M. A., Cheeseman J. R., Zakrzewski V. G., Montgomery J. A., Stratmann R. E., Burant J. C., Dapprich S., Millam J. M., Daniels A. D., Kudin K. N., Strain M. C., Farkas O., Tomasi J., Barone V., Cossi M., Cammi R., Mennucci B., Pomelli C., Adamo C., Clifford S., Ochterski J., Petersson G. A., Ayala P. Y., Cui Q., Morokuma K., Malick D. K., Rabuck A. D., Raghavachari K. , Foresman J. B., Cioslowski J., Ortiz J. V., Baboul A. G., Stefanov B. B., Liu G., Liashenko A., Piskorz P., Komaromi I., Gomperts R. , Martin R. L., Fox D. J., Keith T., Al-Laham M. A., Peng C. Y., Nanayakkara A., Challacombe M., Gill P. M. W., Johnson B., Chen W., Wong M. W., Andres J. L., Gonzalez C., Head-Gordon M., Replogle E. S., Pople J. A., Gaussian 98, Revision A., Gaussian, Inc , ittsburgh PA(1998).

[22] Karamanis P., Pouchan C., (2011), On the shape dependence of cluster (hyper) polarizabilities. A combined ab initio and DFT study on large fullerene–like gallium arsenide semiconductor clusters. *Int. J. Quantum Chem*.111: 788-796.

[23] Hehre W. J., Ditchfield R., Pople J. A., (1972), Self consistent molecular orbital methods. XII. further extensions of Gaussian—type basis sets for use in molecular orbital studies of organic molecules. *J. Chem. Phys*. 56: 2257-2262.

[24] Mattuck R. D., (1967), *A Guide to Feynman Diagrams in the Many-Body Problem*, New York, McGraw-Hill.

[25] Orr B. J., Ward J. F., (1971), Perturbation theory of the non-linear optical polarization of an isolated system. *Moll. Phys*. 20: 513-526.

[26] Guan W., Liu C. G., Song P., Yang G. C., Su Z. M., (2009), Quantum chemical study of redox-switchable second-order optical nonlinearity in Keggin-type organoimido derivative $[PW_{11}O_{39}(ReNC_6H_5)]^{n-}$ (n = 2–4). *Theor. Chem. Account*. 122: 265-273.

[27] Campbell E. E. B., Fanti M., Hertel I. V., Mitzner R., Zerbetto F., (1998), The hyperpolarisability of an endohedral fullerene: $Li@C_{60}$. *Chem. Phys. Lett*. 288: 131-137.

[28] Campbell E. E. B., Couris S., Fanti M., Koudoumas E., Krawez N., Zerbetto F., (1999), Third-order susceptibility of $Li@C_{60}$. *Adv. Mater*. 11: 405-408.

[29] Xie R. H., (1999), Doping effect on the third-order optical nonlinearities of C_{70}. *Phys. Lett. A*. 12: 51-58.

[30] Liu T., Iwata S., Gu B. J., (1994), Structural properties of the endohedral complex $Na^+@C_{60}$.
Phys. Condens. Matter. 6: L253-L258.

[31] Guo T., Jin C., Smalley R. E., (1991), Doping bucky: Formation and properties of boron-doped buckminsterfullerene. *J. Phys. Chem*. 95: 4948-4950.